



Novel Pyrimidinone Linked 1,2,3-Triazole Scaffolds as Anti-Microbial and Antioxidant Agents: Synthesis, *In-vitro* and *In-silico* Studies

**Narendra Kumar Maddali ^a, I. V. Kasi Viswanath ^{b*}, Y. L. N. Murthy ^{c*},
Vasavi Malkhed ^d, Vani Kondaparthi ^e, Pradeep Kumar Brahman ^a
and B. Govindh ^f**

^a Department of Chemistry, Koneru Lakshmaiah Education Foundation (KLEF), Green Fields, Vaddeswaram, Guntur, Andhra Pradesh 522 502, India.

^b Department of Basic Sciences & Humanities (Chemistry), NRIIT, Agiripalle, Vijayawada, Andhra Pradesh 521 211, India.

^c Department of Organic Chemistry, Andhra University, Visakhapatnam, Andhra Pradesh 530 003, India.

^d Molecular Modelling Research Laboratory, Department of Chemistry, Osmania University, Hyderabad, Telangana 500 007, India.

^e Department of Humanities and Sciences, Keshav Memorial Engineering College, Osmania University, Telangana 500058, India.

^f Department of Basic Sciences and Humanities, Raghu Institute of Technology, Visakhapatnam, Andhra Pradesh, India.

Authors' contributions

This work was carried out in collaboration among all authors. All authors read and approved the final manuscript.

Article Information

DOI: 10.9734/JPRI/2021/v33i59A34295

Open Peer Review History:

This journal follows the Advanced Open Peer Review policy. Identity of the Reviewers, Editor(s) and additional Reviewers, peer review comments, different versions of the manuscript, comments of the editors, etc are available here: <https://www.sdiarticle5.com/review-history/79023>

Original Research Article

Received 10 October 2021
Accepted 14 December 2021
Published 16 December 2021

ABSTRACT

The present study states the synthesis of a novel series of pyrimidinone linked 1,2,3-triazole scaffolds by click chemistry method. Further, the synthesized compounds were evaluated for their antimicrobial studies against *S. aureus* and *S. pneumoniae*. Among the synthesized compounds, almost all compounds demonstrated significant antimicrobial activity against *S. aureus*, *S. pneumoniae*, *E.coli* and *P. aeruginosa*, as evident from the zone of inhibition resulted. In addition,

*Corresponding author: E-mail: govindhbd@gmail.com;

synthesised compounds were screened for their antioxidant activity by the 2,2-diphenyl-1-picrylhydrazyl (DPPH) assay method. Furthermore, computational study was performed to understand the interactions between synthesised compounds with dehydroqualene synthase of *Staphylococcus aureus* (PDB ID: 2ZCS) and few Compound revealed the highest binding energies $\Delta G = -9.5, -9.8, \text{ and } -10.1 \text{ Kcal/mol}$.

Keywords: Pyrimidinone; click chemistry; antimicrobial; DPPH; antioxidant; zone of Inhibition.

1. INTRODUCTION

Microbial infections have become a major problem for the world's population and have a significant impact on mortality. These diseases pose a challenge to the scientific community to discover new drugs (antibiotics) to kill microorganisms. The development of broad-spectrum antibiotics plays an important role in the treatment and prevention of infectious diseases. With the use of antibiotics, microbial resistance increased exponentially. Currently, microbial resistance is evolving to multidrug resistance (MDR) due to the abuse of broad-spectrum antibiotics. Antibiotic MDR is a serious public health problem of concern around the world [1-3]. Antibiotic-resistant bacteria continue to develop and spread, dying each year due to a lack of effective antibiotics [4]. Half of the infections caused by bacteria are common to penicillin, methicillin, tetracycline, erythromycin and other antibiotics MDR [5,6]. Therefore, there is a strong need to develop new antibacterial agents to combat MDR.

1,2,3 triazole and its derivatives have received a great deal of attention in recent years due to their

wide range of biological uses, including anti-tuberculosis [7], antibacterial, anti-allergic, anti-HIV [8], antifungal activity [9], and α -glycosidase inhibitor activity [10]. Collected. Available literature shows a wide range of antibacterial activity of 1,2,3 triazole derivatives [11-15]. Also, some containing 1,2,3-triazole moieties such as cefatrizin, tazobactam, 8 rufinamide [16]. Drugs are in clinical trials [15], some of which are future drugs such as carboxylamidotriazole and CAI [17] tert-butyl dimethylsilyl-spyroaminoxathiooxide (TSAO), HIV reverse transcriptase inhibitor [18]. Based on the results of, this study describes the uptake of dihydropyrimidinone [19] and 1,2,3 triazole rings into a compact structure for synergistic effects [20,21]. We also have internal molecules. We are also focusing on docking research. Half of this biologically important class of substances is available for in vitro research, identifying potential research directions for optimizing synthetic lead structures. It has been extended to identify the best candidate among the compounds. In this regard, the integration of the dihydropyrimidinone group with the substituted 1,2,3-triazole unit produces a hybrid molecule (Fig. 1).

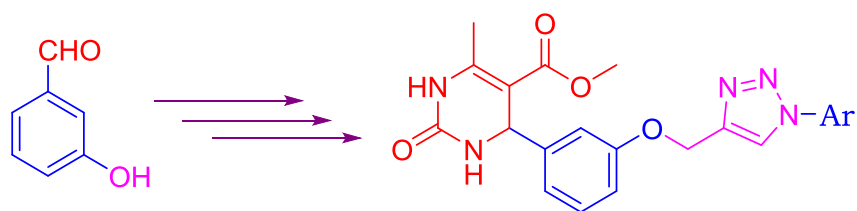


Fig. 1. Design of new pyrimidinone hybrid molecules

2. METHODOLOGY

2.1 Materials

Sigma Aldrich and Merck, both based in India, provided all chemicals and solvents. In the open capillary, the melting point is examined but not corrected. On a TLC plate covered with Kieselgel 60 F254, the reaction was monitored, and spots were spotted using iodine vapor or UV light as a visualizer. The NMR spectra was recorded on a BRUKER Avance DRX400-FT NMR spectrometer at 400 MHz for $^1\text{H-NMR}$ and 100 MHz for $^{13}\text{C-NMR}$, the chemical shift (δ) is in ppm (s=singlet, d=double, t=triplet, q=quartet, quint=quintet, m=multiplet) and the coupling constant (J) is in Hz (s=singlet,

d=double, t= triplet, q=quartet, quint=quintet, m=multiplet). The solvents utilized were deuterated chloroform (CDCl₃) and deuterated dimethyl sulfoxide (d₆-DMSO) from Sigma Aldrich. The FTIR spectrum was recorded on a Shimadzu spectrophotometer at 4000-400 cm. We utilized Merck silica gel 60F254 coated aluminum foil for thin-layer chromatography (TLC). A glass column packed with 60 m silica gel was used for column chromatography. The PerkinElmer Series II CHNS 2400 elemental analyzer was used to conduct the analysis.

2.2 Synthesis

Synthesis of 3-(prop-2-yn-1-yloxy)

Benzaldehyde: In acetonitrile (15-20 ml), a combination of 3-hydroxybenzaldehyde (1.0 mmol), propargyl bromide (1.2 mmol), and K₂CO₃ (1 mmol) were dissolved and agitated at reflux temperature for 5 hours under N₂ atmosphere. TLC is used to track the reaction's progress. Compound 3 was obtained as a yellow liquid in 80-90 percent yield after the solvent was evaporated in vacuo and the residue was purified using silica gel column chromatography eluting with gradient ethyl acetate and n-hexane.

¹H NMR (400 MHz, CDCl₃): δ ppm: 9.9 (s, 1H, -CHO), 7.53–7.45 (comp, 3H, ArH), 7.28–7.24 (m, 1H, ArH), 4.76 (d, J = 2.4 Hz, 2H, OCH₂), 2.56 ppm (t, J = 2.4 Hz, -CH, 1H); ¹³C NMR (100 MHz, DMSO-d₆): δ ppm: 192.1, 158.3, 137.8, 130.2, 124.1, 122.4, 113.4, 78.2, 76.1, 56.3.

Synthesis of Pyrimidinone Derivative (6): 3-(prop-2-yn-1-yloxy)benzaldehyde (1 mmol), methyl acetoester (4) (1 mmol), and urea (5) (1.4 mmol) were refluxed for 3 hours in 5-10 ml of ethanol. TLC is used to monitor the reaction process. The solvent is evaporated in a vacuum, 15 ml of water is added, the product is extracted to ethyl acetate, the generated emulsion is passed through a Celite pad, and ethyl acetate and mixed ethyl acetate are added and washed. The layers were concentrated in vacuo, and the residue was purified using silica gel column chromatography and eluted with gradient ethyl acetate and n-hexane to produce 6 in a yield of 85-90 percent.

¹H NMR (400 MHz, CDCl₃): δ ppm: 2.24 (s, 3H); 3.34 (s, 1H); 3.53 (s, 3H); 4.75 (s, 2H); 5.09 (s, 1H); 6.91-6.93 (m, 2H); 7.14-7.16 (m, 2H); 7.68 (s, 1H); 9.18 (s, 1H); ¹³C NMR (100 MHz, DMSO-d₆): δ ppm: 17.9, 50.8, 53.0, 55.5, 78.2, 79.1, 101.6, 114.2, 114.5, 127.4, 127.8, 137.4, 145.6, 152.3, 165.8, 167.3.

General procedure for the synthesis of final 1,2,3-triazole compounds (8a-i): 2 mmol substituted azide 7a-i (made by reacting each

diazonium salt with sodium azide according to known procedures), appropriate pyrimidinone derivative 6 (2 mmol), copper sulfate (0.5 mmol), and sodium ascorbate (0.5 mmol). The mixture was briskly mixed at room temperature in dry DMF (8 ml). TLC kept track of the reaction's progress on a frequent basis. It was poured into crushed ice after the reaction was finished (40 g). To isolate the pure desired product, the separated particles were filtered off, dried, and purified by column chromatography on silica gel (100-200 mesh) using a gradient combination of ethyl acetate and n-hexane.

Methyl-6-methyl-2-oxo-4-(3-((1-(p-tolyl)-1H-1,2,3-triazol-4-yl)methoxy)phenyl)-1,2,3,4-tetrahydropyrimidine -5-carboxylate(8a)

Pale yellow solid, Yield: 78%; mp: 168-170°C; IR ν_{\max} cm⁻¹: 3229 (NH str), 2945 (CH str), 1696 (CO str), 1554, 1512 (C=C str), 1459 (C=N str), 1245 (N=N str), 1139 (COC str); ¹H NMR (400 MHz, CDCl₃): δ ppm: 8.50 (s, 1H, NH), 8.15 (s, 1H, =CH), 7.81 (s, 1H, ArH), 7.58 (d, 2H, J = 8.2 Hz, ArH), 7.51 (d, 2H, J = 8.0 Hz, ArH), 7.25 (m, 2H, ArH), 6.99 (d, 1H, J = 8.0 Hz, ArH), 5.40 (s, 2H, OCH₂), 4.52 (m, 1H, CH), 4.51 (s, 1H, NH), 3.95 (s, 3H, CH₃), 2.76 (s, 3H, CH₃), 2.27 (s, 3H, CH₃). ¹³C NMR (100 MHz, CDCl₃): δ ppm: 165.4, 160.1, 153.7, 148.6, 145.4, 140.2, 133.5, 131.9, 131.4, 130.4, 129.5, 128.6, 123.6, 122.3, 118.6, 114.8, 98.9, 60.9, 59.4, 55.4, 20.8, 19.2.; ESI-MS (*m/z*): 434(M+H)⁺; Elemental analysis calcd (%) for C₂₃H₂₃N₅O₄: C 63.73, H 5.35, N 16.16; found: C 63.78, H 5.39, N 16.18.

Methyl-4-(3-((1-(4-methoxy-2-nitrophenyl)-1H-1,2,3-triazol-4-yl)methoxy)phenyl)-6-methyl-2-oxo-1,2,3,4-tetrahydropyrimidine-5-carboxylate(8b)

Off white solid, Yield: 75-80%; mp: 128-130°C; IR ν_{\max} /cm⁻¹: 3245br (NH str), 2928w (CH str), 2851w (CH str), 1691s (CO str), 1672s (CO str), 1561, 1512s (C=C str), 1461m (C=N str), 1231m (N=N str), 1085s (COC str); ¹H NMR (400 MHz, DMSO-d₆): δ ppm: 9.16 (s, 1H, NH), 8.71 (s, 1H, =CH), 7.80 (d, 1H, J = 8.8 Hz, ArH), 7.75 (d, 1H, J = 2.7 Hz, ArH), 7.72 (s, 1H, ArH), 7.47 (d, 1H, J = 8.8, ArH), 7.26 (t, 1H, J = 7.8 Hz, ArH), 6.98 (d, 1H, J = 8.0, ArH), 6.83 (m, 1H, NH), 5.17 (s, 2H, OCH₂), 5.11 (d, 1H, J = 3.0 Hz, NH), 3.92 (s, 3H, OCH₃), 2.84 (d, 1H, J = 6.5 Hz,

CH), 2.22 (s, 3H, CH₃), 1.08 (s, 3H, CH₃). ¹³C NMR (100 MHz, CDCl₃): δ ppm 165.9, 160.1, 157.9, 144.7, 144.0, 129.4, 128.9, 119.1, 118.7, 114.4, 113.2, 110.1, 100.4, 59.1, 55.6, 54.3, 17.8, 13.2.; ESI-MS (*m/z*): 495 (M+H)⁺; Elemental analysis calcd (%) for C₂₃H₂₂N₆O₇: C 55.87, H 4.48, N 17.00; found: C 55.94, H 4.54, N 17.28.

Methyl-4-(3-((1-(3-methoxyphenyl)-1H-1,2,3-triazol-4-yl)methoxy)phenyl)-6-methyl-2-oxo-1,2,3,4-tetrahydro pyrimidine-5-carboxylate(8c)

Off white solid, Yield: 72-78%, mp: 171-173°C; IR (KBr) $\nu_{\max}/\text{cm}^{-1}$: 3231br (NH str), 3130br (=CH str), 2941w (CH str), 1699s (CO str), 1598, 1522s (C=C str), 1425m (C=N str), 1231m (N=N str), 1135s (COC str); ¹H NMR (400 MHz, CDCl₃): δ ppm 8.50 (s, 1H, NH), 8.01 (s, 1H, =CH), 7.62 (s, 1H, ArH), 7.41 (dd, 1H, *J* = 8.4, 2.5 Hz, ArH), 7.35 (d, 1H, *J* = 7.5 Hz, ArH), 7.26 (m, 3H, ArH), 7.02 (m, 2H, ArH), 5.40 (s, 2H, OCH₂), 4.52 (d, 1H, *J* = 6.5 Hz, CH), 3.85 (s, 3H, OCH₃), 2.71 (s, 3H, CH₃), 2.10 (s, 3H, CH₃). ¹³C NMR (100 MHz, CDCl₃): δ ppm 164.3, 161.2, 159.6, 153.8, 148.2, 147.5, 142.1, 133.2, 131.9, 131.1, 130.4, 123.8, 121.6, 115.3, 113.4, 110.0, 72.1, 65.6, 53.7, 49.3, 27.1; ESI-MS (*m/z*): 450.0 (M+H)⁺; Elemental analysis calcd (%) for C₂₃H₂₃N₅O₅: C 61.46, H 5.16, N 15.58; found: C 61.54, H 5.29, N 15.65.

Methyl-6-methyl-2-oxo-4-(3-((1-(*m*-tolyl)-1H-1,2,3-triazol-4-yl)methoxy)phenyl)-1,2,3,4-tetrahydropyrimidine-5-carboxylate (8d)

Pale yellow solid, Yield: 79-85%; mp: 158-160°C; IR $\nu_{\max}/\text{cm}^{-1}$: 3241br (NH str), 3139br (=CH str), 2939w (CH str), 1705s (CO str), 1631s (CO str), 1511m (C=C str), 1447m (C=N str), 1238m (N=N str), 1140s (COC str); ¹H NMR (400 MHz, CDCl₃): δ ppm 9.12 (s, 1H, NH), 8.62 (s, 1H, ArH), 8.31 (d, 1H, *J* = 8.5 Hz, ArH), 7.95 (s, 1H, ArH), 7.86 (s, 1H, ArH), 7.31 (dd, 1H, *J* = 8.5, 2.3 Hz, ArH), 7.28-7.25 (m, 1H, ArH), 7.18 (s, 1H, ArH), 6.91 (d, 2H, *J* = 8.5 Hz, ArH), 5.63 (bs, 1H, NH), 5.18 (s, 2H, OCH₂), 3.79 (s, 3H, OCH₃), 2.98 (d, 1H, *J* = 6.5 Hz, CH), 2.28 (s, 3H, CH₃), 1.11 (s, 3H, CH₃). ¹³C NMR (100 MHz, CDCl₃): δ ppm 165.8, 159.9, 158.6, 152.5, 149.1, 145.6, 130.5, 129.5, 121.4, 119.6, 114.9, 113.5, 112.6, 106.1, 101.1, 62.1, 60.1, 55.5, 53.1, 18.6.; ESI-MS (*m/z*): 434 (M+H)⁺; Elemental analysis calcd (%) for C₂₃H₂₃N₅O₄: C 63.73, H 5.35, N 16.16; found: C 63.85, H 5.43, N 16.27.

Methyl-4-(3-((1-(2,5-dimethoxyphenyl)-1H-1,2,3-triazol-4-yl)methoxy)phenyl)-6-methyl-2-oxo-1,2,3,4-tetrahydro pyrimidine-5-

carboxylate(8e) Off white solid, Yield: 75-81%; mp: 180-182°C; IR (KBr) $\nu_{\max}/\text{cm}^{-1}$: 3236(br) (NH str), 3138w (=CH str), 2935w (CH str), 1709s (CO str), 1560, 1511s (C=C str), 1466m (C=N str), 1419m (N=N str), 1231s (COC str), 1139s (COC str); ¹H NMR (400 MHz, DMSO-d₆): δ ppm 9.08 (s, 1H, NH), 8.70 (s, 1H, =CH), 7.77 (d, 1H, *J* = 7.3 Hz, ArH), 7.70 (s, 1H, ArH), 7.63 (d, 1H, *J* = 7.7 Hz, ArH), 7.26-7.24 (m, 1H, ArH), 7.12 (d, 1H, *J* = 7.7 Hz, ArH), 6.97 (d, 1H, *J* = 7.3 Hz, ArH), 6.60 (d, 1H, *J* = 7.8 Hz, ArH), 5.15 (s, 2H, OCH₂), 5.07 (s, 1H, NH), 3.80 (s, 3H, OCH₃), 3.48 (d, 1H, *J* = 6.5 Hz, CH), 3.36 (s, 3H, OCH₃), 2.21 (s, 3H, CH₃), 1.12 (s, 3H, CH₃). ¹³C NMR (100 MHz, CDCl₃): δ ppm 165.9, 160.4, 158.2, 145.5, 144.6, 129.5, 129.3, 119.4, 119.1, 113.6, 110.7, 100.9, 59.8, 56.6, 55.3, 53.4, 18.9; ESI-MS (*m/z*): 480 (M+H)⁺; Elemental analysis calcd (%) for C₂₄H₂₅N₅O₆: C 60.12, H 5.26, N 14.61; found: C 60.24, H 5.35, N 14.73.

Methyl-6-methyl-4-(3-((1-(3-nitrophenyl)-1H-1,2,3-triazol-4-yl)methoxy)phenyl)-2-oxo-1,2,3,4-tetrahydro pyrimidine-5-

carboxylate(8f) White solid, Yield: 65-73%; mp: 150-152°C; IR $\nu_{\max}/\text{cm}^{-1}$: 3148br (NH str), 2925w (CH str), 1707s (CO str), 1689s (CO str), 1586, 1512s (C=C str), 1463m (C=N str), 1267m (N=N str), 1153s (COC str); ¹H NMR (400 MHz, CDCl₃): δ ppm 9.17 (s, 1H, NH), 8.75 (s, 1H, =CH), 7.78 (t, 1H, *J* = 8.3 Hz, ArH), 7.63 (d, 1H, *J* = 7.3 Hz, ArH), 7.58 (s, 1H, ArH), 7.46 (d, 1H, *J* = 7.0 Hz, ArH), 7.17 (m, 2H, ArH), 7.01 (m, 2H, ArH), 5.18 (s, 2H, OCH₂), 5.13 (d, 1H, *J* = 6.5 Hz, CH), 4.61 (s, 1H, NH), 3.95 (s, 3H, CH₃), 2.20 (s, 3H, CH₃). ¹³C NMR (100 MHz, DMSO-d₆): δ ppm 166.7, 160.1, 158.2, 152.5, 148.2, 147.6, 144.3, 130.1, 123.5, 122.4, 119.3, 116.4, 114.7, 100.0, 68.6, 59.8, 55.6, 18.2; ESI-MS (*m/z*): 465 (M+H)⁺; Elemental analysis calcd (%) for C₂₂H₂₀N₆O₆: C 56.90, H 4.34, N 18.10; found: C 56.99, H 4.41, N 18.23.

Methyl-4-(4-((1-(4-methoxyphenyl)-1H-1,2,3-triazol-4-yl)methoxy)phenyl)-6-methyl-2-oxo-1,2,3,4-tetrahydro pyrimidine-5-

carboxylate(8g) Off white solid, Yield: 78-82%; mp: 184-186°C; IR ($\nu_{\max}/\text{cm}^{-1}$): 3221br (NH str), 3104w (=CH str), 2931w (CH str), 1699s (CO str), 1631s (CO str), 1521s (C=C str), 1457m (C=N str), 1241m (N=N str), 1136s (COC str); ¹H NMR (400 MHz, CDCl₃): δ ppm 8.60 (s, 1H, NH), 8.51 (s, 1H, NH), 8.29 (s, 1H, =CH), 8.17 (m, 2H, ArH), 8.11 (s, 1H, ArH), 7.72 (m, 2H, ArH), 7.38 (d, 1H, *J* = 9.0 Hz, ArH), 7.12 (d, 1H, *J* = 9.0 Hz, ArH), 6.91 (d, 1H, *J* = 9.0 Hz, ArH), 5.05 (s, 2H, OCH₂), 3.87 (s, 3H, OCH₃), 2.98 (d,

1H, $J = 6.5$ Hz, CH), 2.33 (s, 3H, CH₃), 1.16 (s, 3H, CH₃). ¹³C NMR (100 MHz, DMSO-d₆): δ ppm166.0, 160.1, 158.3, 152.8, 149.7, 146.7, 144.8, 131.1, 130.2, 123.9, 122.4, 119.1, 115.9, 113.8, 99.5, 60.6, 58.5, 56.1, 53.5, 18.5; ESI-MS (m/z): 450 (M+H)⁺; Elemental analysis calcd (%) for C₂₃H₂₃N₅O₅: C 61.46, H 5.16, N 15.58; found: C 61.50, H 5.22, N 15.63.

Methyl-6-methyl-4-(4-((1-(2-nitrophenyl)-1H-1,2,3-triazol-4-yl)methoxy)phenyl)-2-oxo-1,2,3,4-tetrahydropyridine-5-carboxylate(8h) White solid, Yield: 65-75%; mp: 180-182°C; IR $\nu_{\max}/\text{cm}^{-1}$: 3242br (NH str), 3104br (=CH str), 2934w (CH str), 1692s (CO str), 1631s (CO str), 1523s (C=C str), 1456m (C=N str), 1243m (N=N str), 1137s (COC str); ¹H NMR (400 MHz, CDCl₃) δ 9.10 (s, 1H, NH), 8.12 (s, 1H, =CH), 8.04 (s, 1H, ArH), 7.83 (t, 1H, $J = 7.3$ Hz, ArH), 7.72 (t, 1H, $J = 7.3$ Hz, ArH), 7.63 (d, 1H, $J = 6.3$ Hz, ArH), 7.52 (s, 1H, ArH), 7.20 (d, 1H, $J = 7.7$ Hz, ArH), 6.97 (m, 2H, ArH), 5.96 (s, 1H, NH), 5.30 (s, 2H, OCH₂), 3.45 (d, 1H, $J = 6.5$ Hz, CH), 2.33 (s, 3H, CH₃), 1.63 (s, 3H, CH₃); ¹³C NMR (100 MHz, CDCl₃): δ ppm166.3, 158.0, 145.4, 144.6, 137.3, 129.9, 120.3, 119.1, 114.2, 110.8, 99.3, 56.1, 55.3, 53.1, 18.3; ESI-MS (m/z): 465 (M+H)⁺; Elemental analysis calcd (%) for C₂₂H₂₀N₆O₆: C 56.90, H 4.34, N 18.10; found: C 57.21, H 4.41, N 18.29.

Methyl-4-(4-((1-(4-chlorophenyl)-1H-1,2,3-triazol-4-yl)methoxy)phenyl)-6-methyl-2-oxo-1,2,3,4-tetrahydropyridine-5-carboxylate (8i) Pale yellow solid, Yield: 70-80%; mp: 145-147°C; IR (KBr) $\nu_{\max}/\text{cm}^{-1}$: 3239br (NH str), 2922w (CH str), 2845w (CH str), 1715s (CO str), 1681s (CO str), 1589, 1515s (C=C str), 1460m (C=N str), 1261m (N=N str), 1155s (COC str), 826s (CCI str); ¹H NMR (400 MHz, CDCl₃): δ 8.28 (s, 1H, NH), 7.80 (s, 1H, =CH), 7.46 (d, 1H, $J = 6.5$ Hz, ArH), 7.25 (d, 2H, $J = 7.6$ Hz, ArH), 6.98 (m, 3H, ArH), 6.97 (d, 2H, $J = 7.6$ Hz, ArH), 5.22 (s, 2H, OCH₂), 5.15 (d, 1H, $J = 5.5$ Hz, CH), 3.95 (s, 3H, CH₃), 2.39 (s, 3H, CH₃). ¹³C NMR (100 MHz, CDCl₃): δ ppm166.1, 162.2, 161.1, 158.2, 152.3, 151.0, 145.3, 131.6, 130.8, 121.9, 120.5, 115.6, 114.1, 113.8, 106.7, 69.2, 56.5, 54.2, 18.5; ESI-MS (m/z): 455(M+H)⁺; Elemental analysis calcd (%) for C₂₂H₂₀ClN₅O₄: C 58.22, H 4.44, N 15.43; found: C 58.29, H 4.51, N 15.46.

2.3 Biological Studies

2.3.1 Antibacterial activity

The antibacterial activity of synthesized substances was tested using the disc diffusion

method against the pathogens listed below [22]. *Staphylococcus aureus* and *Streptococcus pneumoniae* were the Gram-positive bacteria tested, whereas *Escherichia coli* and *Pseudomonas aeruginosa* were the Gram-negative bacteria. DMSO was employed as the solvent and the produced chemical was used at doses of 50, 100, and 250 g / ml. As a benchmark, ciprofloxacin is employed. At 45°C, a suspension of *Staphylococcus aureus* (SA) was added to a sterile nutritional agar medium, which was then transferred to a sterile Petri dish and solidified to a depth of 3-4 mm. The homogenous layer of medium on the plate has been seen to be reduced by preparations. Untreated control samples were stored for comparison after dipping a 5 mm diameter sterile disc (made of Whatman filter paper) in a solution of the produced chemical (250 g / ml). To reduce variability at other times, leave the plate at room temperature for 1 hour as a pre-incubation diffusion time. After that, the plate was incubated for 24 hours at 37°C to test its antibacterial activity. For each plate, the diameter of the inhibitory zone was measured. The standard zone and the mean zone of inhibition were determined and compared. Antibacterial activity against different organisms was studied using a similar method.

2.3.2 Antioxidant activity methodology

Sigma Aldrich provided chemicals for in-vitro antioxidant activity of 2,2-Diphenyl-1-Picryl hydroxyl (DPPH) (Bangalore, India). All other reagents and chemicals were analytical reagent quality, except dimethylsulfoxide (DMSO) and methanol, which were HPLC grade. Based on the stable DPPH free radical scavenging activity, [23,24] the antioxidant activity of the finished product and the standard (ascorbic acid) were assessed. The following is a list of the ten liters of each test substance or standard (0.0-1000 M/mL). In a 96-well microtiter plate, 90 L was added to a 100 M methanol solution of DPPH. An ELISA microplate reader was used to measure the decrease in absorbance of each solution at 517 nm after 30 minutes of incubation at 37°C in the dark. Blank samples containing the same amount of DMSO and DPPH solutions were also made and tested for absorbance. All of the experiments were repeated three times. The scavenging potential was compared to solvent control (no radical scavenger) and reference compounds. The following equation was used to compute the radical scavenging activity:

$$\% \text{ Reduction of absorbance} = [(AB - AA) / AB] \times 100$$

AB – absorbance of blank sample and AA – absorbance of tested compound (t = 30 min).

2.4 Computational Studies

2.4.1 Docking methodology

Identification of Active Site Pockets: The internet service tool PdbSum [25] was used to make active site predictions. Two hydrogen bond interactions are found in the active site, and the amino acids His18 and Tyr41 are present. The ligand tripotassium-(1r)-4-biphenyl-4-yl-1-phosphonatobutane sulfonate crystallises the protein 2ZCS. ChemSketch (ACD / ChemSketch, version 2020.1.2, Advanced Chemistry Development, Inc., Toronto, Ontario, Canada, www.acdlabs.com, 2020) was used to draw nine synthetic compounds, which were then converted to mol² format using OpenBabel. We performed individual molecular docking studies on all nine ligands and incorporated an empirical free energy assessment feature using the AutoDock 4.2 programme [26-29] with the Lamarck Genetic Algorithm (LGA). 11 RCSB (<https://www.rcsb.org/structure/2zcs>) was the source of this protein [30,40]. Protein database AutoDock will upload it, hydrogen will be added afterwards, and it will be saved in the PDBQT format. The ligands were then loaded one by one, their conformations were determined, and they were saved in PDBQT format. The automatic grid was used to choose and calculate the grid parameters. For all docking studies, a gridpoint spacing of 0.375 was adopted. The grid map comprised 60x60x60 points in size. The active site amino acids were used to determine the X, Y, and Z coordinates. The default AutoDock parameters have been configured. Docking interactions are visualized with BIOVIA Discovery Studio Visualizer (Discovery Studio Visualiser v 19.1.0.18287).

Methodology of Absorption Distribution, Metabolism and Excretion (ADME) Properties:

The pharmacokinetic properties of the ligand molecule 8a-8i are predicted using the online server tool SwissADME. Physicochemical, pharmacokinetic, lipophilic, and drug-like properties are evaluated for the molecule to reduce clinical failure [31-35].

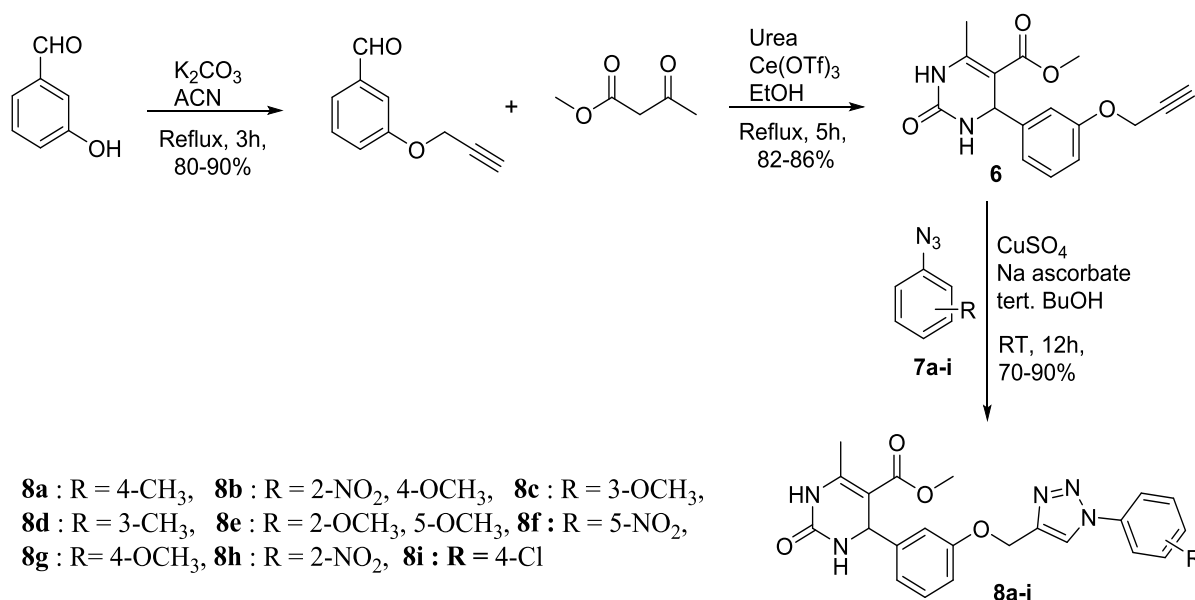
3. RESULTS AND DISCUSSION

3.1 Chemistry

The goal of this research is to develop new pyrimidinone-conjugated 1,2,4-triazole derivatives, as well as to conduct biological evaluations and docking studies to better understand compound-protein interactions. The necessary 3-(prop-2-yn-1-yloxy)benzaldehyde is obtained via O-alkylation of 3-hydroxybenzaldehyde with propargyl bromide and K₂CO₃ to afford the required 3-(prop-2-yn-1-yloxy) benzaldehyde [36]. Further treatment of compound 3 with methyl acetoacetate and urea results methyl 6-methyl-2-oxo-4-(3-(prop-2-yn-1-yloxy)phenyl)-1,2,3,4-tetrahydropyrimidine-5-carboxylate (6). [37-38] In the presence of CuSO₄·5H₂O and Na-ascorbate in dry DMF, the terminal alkyne derivatives (6) and 7 (a-i) were transformed to 8 (a-i) in 70-85% yield (scheme 1). ¹H-NMR, ¹³C-NMR, IR, MS, and elemental analyses were used to confirm all produced compounds. The antibacterial and antioxidant characteristics of the compounds created were studied in order to discover potent molecules.

3.2 Antibacterial Activity

In vitro antibacterial activity against gramme (+) pathogens was investigated on 8 (a-i) compounds. mm. Using ciprofloxacin as a reference medication (Table 1). The antibacterial activity of the pyrimidinone-targeted triazoles 8e, 8f, and 8h demonstrated outstanding broad-spectrum activity against the representative gramme (+) and gramme (-) germs, according to the results of the in-vitro assay. Against the organisms examined, all of the synthesized compounds 8 (a-i) demonstrated high antibacterial activity. The Gram-positive bacterium *Staphylococcus aureus* was inhibited by compounds 8e, 8f, and 8h, with inhibition zones of 18, 17, and 17 mm, respectively. With inhibition zones of 18, 16, and 16 mm, the three compounds 8a, 8e, and 8h exhibited good effectiveness against *Streptococcus pneumoniae* strains. Compounds 8d, 8e, and 8f have greater action against *Pseudomonas aeruginosa* in inhibition zones of 20, 18, and 17 mm, respectively, as well as *E. coli*, a gram-negative bacterium. Showed a lot of energy. Furthermore, as compared to ciprofloxacin, the final target triazole in combination with dihydropyrimidinone



Scheme 1. Synthesis of novel 1,2,3-triazols linked pyrimidinone scaffolds

8e, 8f, and 8h demonstrated higher action against all Gram-positive and Gram-negative bacteria. *Pseudomonas aeruginosa*, *Staphylococcus aureus*, *pneumonia*, and *Pseudomonas aeruginosa* were all found to be more efficient against freshly manufactured hybrids. *E. coli* is a type of bacteria. SAR analysis revealed that terminal compounds having substituents at the meta-position of the benzene ring, such as NO₂, Cl, and OMe, had the best antibacterial activity.

3.3 Antioxidant Activity

Table 1 shows the antioxidant activity data of the synthesized framework 8 (ai). The results show that all compounds have a strong antioxidant activity profile. Of all synthesized 4-methoxyphenyl 1,2,3 triazole and dihydropyrimidinone (8g), 2-nitrophenyl 1,2,3 triazole and dihydropyrimidinone (8h) and 2, 5-Dimethoxyphenyl 1,2,3 triazole and dihydropyrimidinone (8e) have the highest antioxidant activity (80%, 59% and 51% at 1 mg mL⁻¹ concentration), with an IC₅₀ value of 320 µg mL. It is -1 (1.42 mM). Compounds 8b, 8f and 8i show moderate antioxidant activity (44-50%). It is worth noting that the antioxidant capacity of compound 8 g may have already been observed at lower concentrations (750, 500, 250, and 125 µg mL⁻¹). It was found that the DPPH scavenger potential at 8 g and 8 hours decreased with

increasing concentration. The effectiveness of 8 g against other compounds in the elimination of DPPH activity demonstrates the importance of the 1,2,3-triazole moiety in enhancing the antioxidant capacity of dihydropyrimidinone.

3.4 Docking Study

The capacity of the new compounds to bind at the active site of the *Staphylococcus aureus* protein with PDB ID 2ZCS were evaluated for their mode of action of dehydrosqualene synthase. PdbSum tool analysis yielded a grid at the active site residues HIS18, PHE22, TYR41, ARG45, ALA134, VAL137, LEU141, ALA157, LEU160, LEU164, ILE241, and TYR248. Molecular docking is the most frequent approach for calculating protein-ligand interactions, and it is also a potent way of forecasting possible ligand interactions. Antibacterial protein inhibition was performed using Vina software and AutoDock 4.2 for the foreign compounds chosen for study. Docking analysis determines the binding free energy and predicts the optimal binding confirmation for the ligands 8 that fits into the receptor (a-i). The produced compounds were docked with dehydrosqualene synthase complexed with the crystal structure of Tripotassium(1r)-4-biphenyl-4-yl-1-phosphonatobutane-1-sulfonate ligand (PDB ID:2ZCS) [39].

Table 1. Antibacterial (inhibition of zone (mm)) and Antioxidant activity of compounds (8a-i)

Compound	Gram + ve bacteria		Gram - ve bacteria		DPPH Scavenging (%) ^b
	<i>S. aureus</i>	<i>S. pneumoniae</i>	<i>E. coli</i>	<i>P. aeruginosa</i>	
8a	15±0.1	16±0.3	12±0.2	16±0.3	28
8b	16±0.2	13±0.3	15±0.2	14±0.1	49
8c	14±0.1	15±0.3	15±0.2	13±0.3	18
8d	15±0.2	14±0.1	16±0.3	17±0.2	20
8e	18±0.1	16±0.2	17±0.2	18±0.3	51
8f	17±0.2	15±0.1	14±0.2	20±0.3	44
8g	15±0.2	14±0.3	15±0.1	18±0.2	80
8h	17±0.2	18±0.1	16±0.3	14±0.2	59
8i	15±0.3	12±0.3	14±0.4	15±0.2	50
Standard	30±0.1 ^a	33±0.3	34±0.1	28±0.2	93 ^c

Antibacterial activity results are the mean \pm SD; n=6, ^aCiprofloxacin used as standard; ^bAntioxidant results are the mean of three different experiments, ^cAscorbic acid used as standard

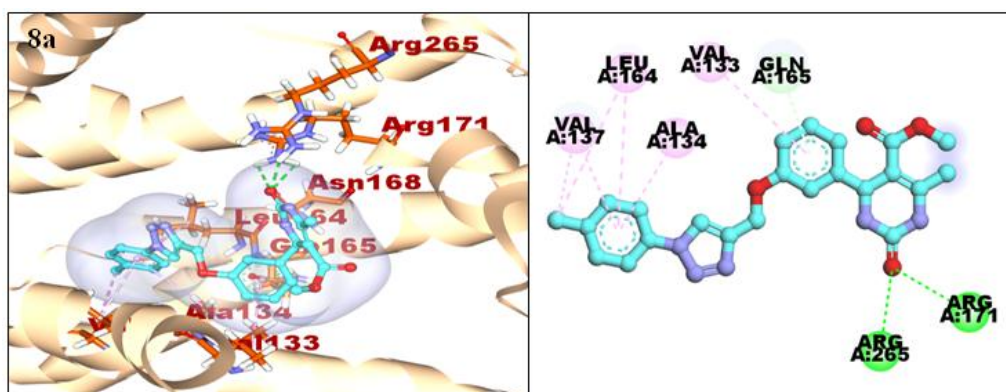
Table 2 shows that all of the compounds had the highest binding energies and multiple amino acid interactions with the protein 2ZCS. Eight chemicals interact with one of three amino acids, according to docking results: ARG45, ASP 48, TYR129, GLN165, ASN 168, ARG171, ARG 181TYR183, and ARG265. The amino acids ARG45, TYR129, and GLN165 of the 2ZCS protein interact with the molecules 8b, 8d, and 8h. The resulting compounds had good binding values and dissociation constants ranging from G = -8.1 to -10.1 kcal/mol and 1.39 to 596.68 M, respectively (Table 2).

When interacting with the amino acids ARG45, TYR129, GLN165, ASN168, ARG171, ILE241, TYR248, and ARG265, compounds 8a, 8h, and 8i have the highest binding energies of -9.5, -9.8, and -10.1 Kcal/mol. The greatest dissociation constant values are 596.68, 277.51, 252.57, and 252.53M for the docking conformations of the ligands 8i, 8b, 8g, and 8d, respectively. Because it is bonded with more non-bonded contacts with the receptor amino acids, molecule 8i has the highest dissociation constant value. All the molecules 8a-8i exhibited good binding energy

values. Fig. 2; i) and ii) represents the complexes of dehydroqualene synthase (2ZCS) with the compounds 8(a-f) ligands interactions in 3D and 2D representations. All the molecules are forming in common one π - π stacking bond with the phenyl ring of PHE22 residue of the 2ZCS protein.

3.5 ADME Properties

The ADME properties predicted by all frameworks 8 (a-i) are acceptable (Table 3 and Fig. 3). All ligand molecules contain two hydrogen bond donors. All molecules except NO₂-substituted 8b, 8f, and 8h ligand molecules have high G_i absorption, indicating that all molecules can be orally administered. Molecules 8b and 8f are positive substrates for permeable glycoprotein (Pgp) and have no human gastrointestinal absorption [40]. All molecules are considered good drug molecules according to Lipinski's Rule 5. The molecule does not interact with some cytochrome P450 isoforms and confirms that their metabolites have been removed.



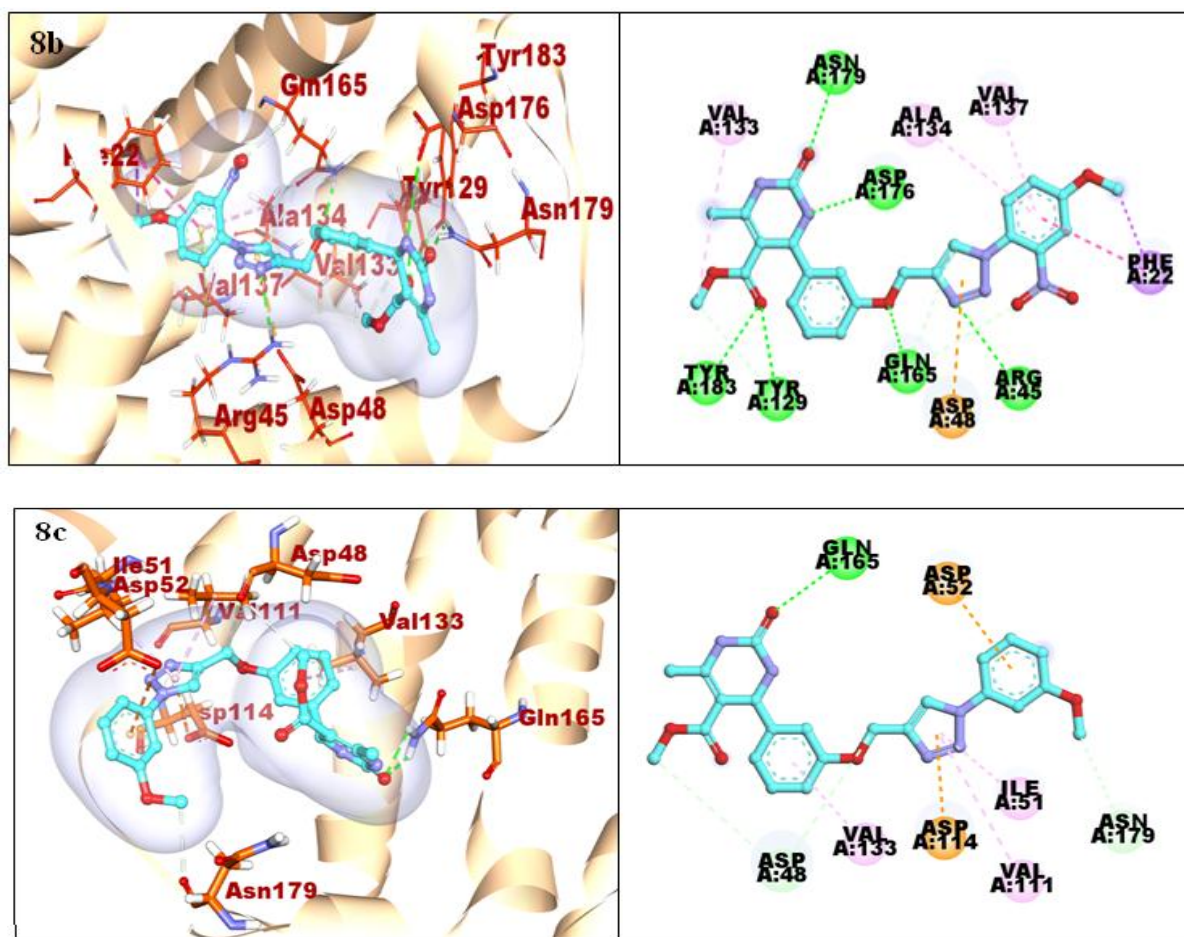


Fig. 2. The binding interactions between PDB ID 2ZCS protein with the ligand scaffolds 8(a-c)

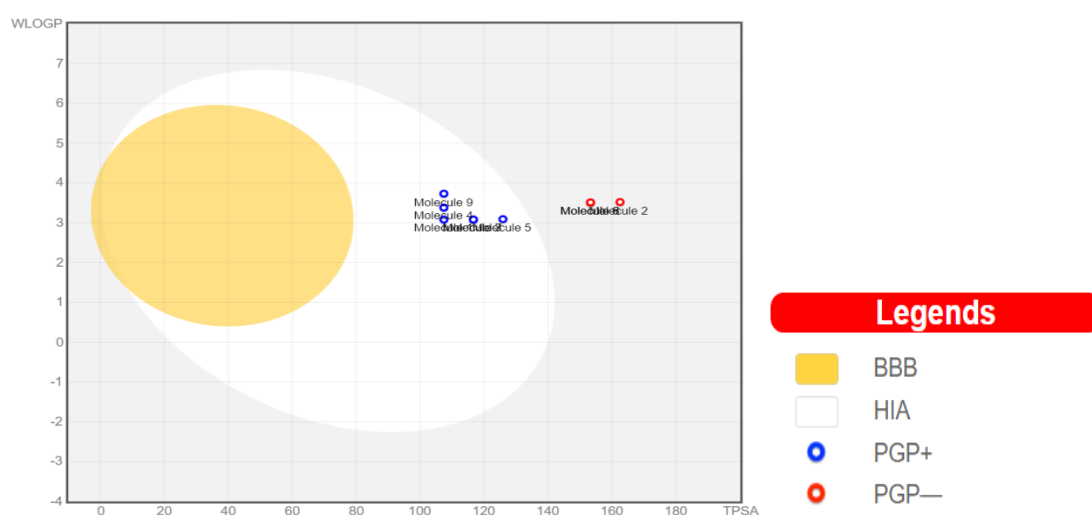


Fig. 3. Plot of total polar surface area (TPSA) and WlogP for the ligands 8(a-i)
 In Fig. 3 Each molecule is represented with a dot in the graph. The molecules do not cross the blood-brain barrier and fall in the range of oral bioavailability limits. (BBB-blood brain barrier, HIA- Human gastrointestinal absorption, PGP- Permeability glycoprotein)

Table 2. List of docking interaction distances (Å) along with the docking energies (kcal/mole) and dissociation constant (µM) values for each ligand 8(a-i) docked with dehydroqualene synthase (PDB ID: 2ZCS) (Bond distances less than 4 Å are presented)

Ligand	Docking Energy (ΔG)	Dissociation constant (KI)	Interacting Amino acid Residues	Bond distance
8a	-9.5	16.95	Hydrogen Bond	
			ARG171:HH21 -8a:O10	2.850
			ARG171:HH22 - 8a:O10	2.966
			ARG265:HH22 - 8a:O10	2.417
			GLN165:HE22 - :8a	2.751
8b	-9	277.51	Hydrogen Bond	
			8b:N11 -ASP176:OD2	3.226
			ARG45:HH21 - 8b:N23	2.505
			TYR129:HH - 8b:O1	2.339
			GLN165:HE22 - 8b:O20	2.255
			ASN179:HD21 - 8b:O10	2.207
			TYR183:HH - 8b:O1	2.224
			8b:C26 - GLN165:OE1	3.311
			8b:C4 :TYR129:OH	3.523
			GLN165:HA - 8b:O35	3.032
			π -anion	
			ASP48:OD2 - :8b	3.871
			π -sigma	
8b:C37 - PHE22	3.760			
8c	-8.1	20.04	Hydrogen Bond	
			GLN165:HE21 - 8c:O10	2.706
			GLN165:HE22 - 8c:O10	2.612
			ASN168:HD21 - 8c:O10	2.726
			8c:C21 - ASP48: O	3.488
			8c:C34 -ASN179: O	3.379
			8c:C4 - ASP48: O	3.783
			π -anion	
ASP114:OD1 - :8c	3.324			

Ligand	Docking Energy (ΔG)	Dissociation constant (KI)	Interacting Amino acid Residues	Bond distance
8d	-9.4	252.53	Hydrogen Bond	
			8d:N11:TYR129:OH	3.057
			ARG45:HH21 - :8d:N23	2.742
			ARG45:HH22 - :8d:O1	2.450
			ASN168:HD22 - 8d:O20	2.910
8d:C26 :GLN165:OE1	3.341			
8e	-8.7	3.96	Hydrogen Bond	
			ARG45:HH22 - :8e:O3	2.269
			ARG181:HE - :8e:O10	2.453
8f	-9.1	8.10	Hydrogen Bond	
			ARG45:HH21 - :8f:N23	2.666
			ASN168:HD22 - :8f:O20	2.342
			ARG181:HE - :8f:O10	2.600
			HIS18:HE1 - :8f:N23	3.032
8g	-9.3	252.57	Hydrogen Bond	
			ARG45:HH22 - :8g:O1	2.575
			ASN168:HD22 - :8g:O10	2.607
			8g: C34:ALA157: O	3.578
8g:C4:TYR129:OH	3.640			
8h	-9.8	1.65	Hydrogen Bond	
			8h:N11 - TYR129:OH	3.044
			ARG45:HH21 - 8h:N23	2.322
			ASN168:HD22 -8h:O20	2.816
			TYR248:HH - 8h:O34	2.342
			8h:C26 - GLN165:OE1	3.603
			HIS18:HE1 - 8h:N23	3.098
GLN165:HA - 8h:O35	2.798			

8i	-10.1	596.68	Hydrogen Bond ARG45:HH21 - 8i:O1 ARG171:HH12 - 8i:O10 alkyl 8i:CL33:ILE241 π -alkyl PHE233 :8i:CL33	2.742 2.426 3.889 3.993
-----------	-------	--------	---	----------------------------------

Table 3. Predicted ADME properties for the ligands 8(a-i)

Molecule	Molecule No	MW	Lipinski rule	Rotatable bonds	HB acceptors	HB donors	TPSA	WLOGP	GI absorption	iLOGP	Lead likeness
8a	Molecule 1	495.5	0	8	6	2	107.37	3.08	High	3.55	3
8b	Molecule 2	570.5	2	10	9	2	162.42	3.52	Low	3.63	2
8c	Molecule 3	525.5	1	9	7	2	116.6	3.08	High	4.33	3
8d	Molecule 4	509.5	1	8	6	2	107.37	3.38	High	4.26	3
8e	Molecule 5	555.5	2	10	8	2	125.83	3.09	High	4.56	3
8f	Molecule 6	540.5	2	9	8	2	153.19	3.51	Low	3.66	2
8g	Molecule 7	525.5	1	9	7	2	116.6	3.08	High	3.97	3
8h	Molecule 8	540.5	2	9	8	2	153.19	3.51	Low	3.48	2
8i	Molecule 9	529.9	1	8	6	2	107.37	3.73	High	4.1	3

4. CONCLUSIONS

Finally, the research concentrated on the synthesis of a new series of phenyl substituted 1,2,3-triazoles linked to 1,2,3,4-tetrahydro pyrimidine heterocyclic rings 8(a-i), with spectrum analysis confirming the structures. Gram-(+ve) and Gram-(-ve) bacteria were tested for representative compounds of the produced products, and 8a, 8e, and 8h compounds were evaluated as possible antimicrobial agents. When compared to ascorbic acid (93%), the triazole functionalized compounds 8e, 8g, and 8h had the highest antioxidant activity, with inhibition of 80%, 59%, and 51%. The maximum binding energy, hydrogen bonding, Van der Waal forces, and π -stacking were also found in the molecular docking data of produced compounds. The ADME properties of the synthesized compounds are predicted, and the study revealed that the values determined for 8(a-i) are within druggable molecules' acceptable limits. The novel pyrimidinone hybrid compounds could be used as lead molecules in the development of new antibacterial and antioxidant chemicals.

DISCLAIMER

The products used for this research are commonly and predominantly use products in our area of research and country. There is absolutely no conflict of interest between the authors and producers of the products because we do not intend to use these products as an avenue for any litigation but for the advancement of knowledge. Also, the research was not funded by the producing company rather it was funded by personal efforts of the authors.

CONSENT

It is not applicable.

ETHICAL APPROVAL

It is not applicable.

ACKNOWLEDGEMENTS

The authors are very much thankful to KLEF (Deemed to be University) management for their immense support. The authors KV and

MV are thankful to the Molecular modelling research laboratory Department of Chemistry, the Head, Department of Chemistry, and the Principal, University College of Science, Osmania University, for providing the facilities to carry out the computational work.

COMPETING INTERESTS

Authors have declared that no competing interests exist.

REFERENCES

1. Joule JA, Mills K 2013 Heterocyclic Chemistry (London: John Wiley)
2. De Oliveira CGM, Faria VW, de Andrade GF, D'Elia E, Cabral MF, Cotrim BA. Sulfur, and Silicon and the Related Elements. Synthesis of Thiourea Derivatives and its Evaluation as Corrosion Inhibitor For Carbon Steel. Phosphorus, Sulfur, and Silicon and the Related Elements.2015;190:1366. Available:<https://doi.org/10.1080/10426507.2015.1035719>
3. Yoneyama H, Katsumata R, Biosci. Biotechnol. Antibiotic Resistance in Bacteria and Its Future for Novel Antibiotic Development. Biosci. Biotechnol. Biochem Biochem. 2006; 70:1060. Available:<https://doi.org/10.1271/bbb.70.1060>
4. Lim SM, Webb SAR. Nosocomial bacterial infections in Intensive Care Units. I: Organisms and mechanisms of antibiotic resistance. Anaesthesia2005;60:887.. Available:<https://doi.org/10.1111/j.1365-2044.2005.04220.x>
5. Grundmann H, Aires-de-Sousa M, Boyce J, Tiemersma E. Emergence and resurgence of meticillin-resistant Staphylococcus aureus as a public-health threat. Lancet. 2006;368:874.. Available:[https://doi.org/10.1016/S0140-6736\(06\)68853-3](https://doi.org/10.1016/S0140-6736(06)68853-3).
6. Aufort M, Herscovici J, Bouhours P, Moreau N, Girard C. Synthesis and antibiotic activity of a small molecules library of 1,2,3-triazole derivatives. . Bioorg. Med. Chem. Lett. 2008; 18:1195. Available:<https://doi.org/10.1016/j.bmcl.2007.11.111>

7. Boechat N, Ferreira VF, Ferreira SB, de Lourdes GFM, de CdSF, Bastos MM et al. Novel 1,2,3-triazole derivatives for use against Mycobacterium tuberculosis H37Rv (ATCC 27294) strain. *J.Med. Chem.* 2011;54:5988. Available:<https://doi.org/10.1021/jm203624>
8. Agalave SG, Maujan SR, Pore VS. Click Chemistry: 1,2,3-Triazoles as Pharmacophores. *Chem. Asian J.* 2011;6:2696. Available:<https://doi.org/10.1002/asia.201100432>
9. Lima-Neto RG, Cavalcante NNM, Srivastava RM, Mendonça Junior FJB, Wanderley AG, Neves RP et al. Synthesis of 1,2,3-Triazole Derivatives and in Vitro Antifungal Evaluation on Candida Strains. *Molecules.* 2012; 17:5882. Available:<https://doi.org/10.3390/molecules17055882>
10. Senger MR, Gomes LdCA, Ferreira SB, Kaiser CR, Ferreira VF, Silva Jr FP 2012 Kinetics Studies on the Inhibition Mechanism of Pancreatic α -Amylase by Glycoconjugated 1H- 1,2,3-Triazoles: A New Class of Inhibitors with Hypoglycemic Activity. *ChemBioChem.* 2012;13:1584. Available:<https://doi.org/10.1002/cbic.201200272>
11. Reddy KI, Srihari K, Renuka J, Sree KS, Chuppala A, Jeankumar VU et al. An efficient synthesis and biological screening of benzofuran and benzo[d]isothiazole derivatives for Mycobacterium tuberculosis DNA GyrB inhibition. *Bioorg. Med.Chem.*2014;22:6552. Available:<https://doi.org/10.1016/j.bmc.2014.10.016>
12. Krivopalov VP, Shkurko OP. 1,2,3-Triazole and its derivatives. Development of methods for the formation of the triazole ring *Russ. Chem. Rev.* 2005;74:339. Available:<https://doi.org/10.1070/RC2005v074n04ABEH000893>
13. Albert Padwa. 1,3-dipolar Cycloaddition Chemistry. NY, John Wiley & Sons. 1986;1 and 2.
14. Whiting M, Muldoon J, Lin Y-C, Silverman SM, Lindstrom W, Olson AJ et al. Inhibitors of HIV-1 Protease by Using In Situ Click Chemistry *Angew.Chem. Int. Ed.*, 2006;45:1435.. Available:<https://doi.org/10.1002/anie.200502161>
15. Horne WS, Yadav MK, Stout CD, Ghadiri MR. Heterocyclic Peptide Backbone Modifications in an α -Helical Coiled Coil. *J. Am. Chem. Soc.* 2004;126:15366 Available:<https://doi.org/10.1021/ja0450408>
16. Johannessen Landmark C, Patsalos PN. Drug interactions involving the new second and third-generation antiepileptic drugs. *Expert Rev. Neurother.* 2010;10:119. Available:<https://doi.org/10.1586/ern.09.136>
17. Guo L, Ye C, Chen W, Ye H, Zheng R, Li J et al. Anti-inflammatory and analgesic potency of carboxyamidotriazole, a tumorostatic agent. *J. Pharmacol. Exp. Ther.* 2008;325:10. Available:<https://doi.org/10.1124/jpet.107.131888>
18. De Clercq E. HIV resistance to reverse transcriptase inhibitors. *Pharmacol.* 1994;47:155. Available:[https://doi.org/10.1016/0006-2952\(94\)90001-9](https://doi.org/10.1016/0006-2952(94)90001-9)
19. Farooq S, Alharthi FA, Alsalmeh A, Hussain A, Dar BA, Hamid A et al. Dihydropyrimidinones: efficient one-pot green synthesis using Montmorillonite-KSF and evaluation of their cytotoxic activity. *RSC Adv.* 2020;10:42221. Available:<https://doi.org/10.1039/d0ra09072g>
20. Adigun RA, Malan FP, Balogun MO, October N. J. Substitutional effects on the reactivity and thermal stability of dihydropyrimidinones. *N. J. Mol. Struct.* 2021;1223:129193. Available:<https://doi.org/10.1016/j.molstruc.2020.129193>
21. Shaik K, Faraat A, Kiran M, Anjali S, Garima C, Sharad W. Dihydropyrimidinones Scaffold as a Promising Nucleus for Synthetic Profile and Various Therapeutic Targets: A Review. *Curr. Org. Synth.* 2021;18:270. Available:<https://doi.org/10.2174/1570179417666201207215710>

22. Kumar SS, Kamaraj M. Analysis of phytochemical constituents and antimicrobial activities of *Cucumis anguria* L. against clinical pathogens. *J. Agric. & Environ. Sci.* 2010;7:176.
23. Brader G, Vajrodaya S, Greger H, Bacher M, Kalchhauser H, Hofer O. Bisamides, Lignans, Triterpenes, and Insecticidal Cyclopenta[b]benzofurans from *Aglaia* Species. *J. Nat. Prod.* 1998;61:1482.
Available:<https://doi.org/10.1021/np9801965>
24. Liu L, Sun Y, Laura T, Liang X, Ye H, Zeng X. Determination of polyphenolic content and antioxidant activity of kudingcha made from *Ilex kudingcha* C.J. Tseng. *Food Chem.* 2009;112:35.
Available:<https://doi.org/10.1016/j.foodchem.2008.05.038>
25. Laskowski RA. PDBsum new things. *Nucleic Acids Res.* 2009;37:D355.
Available:<https://doi.org/10.1093/nar/gkn860>
26. Morris GM, Huey R, Lindstrom W, Sanner MF, Belew RK, Goodsell DS et al. AutoDock4 and AutoDockTools4: Automated docking with selective receptor flexibility. *J. Comput.Chem.* 2009;30:2785.
Available:<https://doi.org/10.1002/jcc.21256>
27. Trott O, Olson AJ. 2010 AutoDock Vina: Improving the speed and accuracy of docking with a new scoring function, efficient optimization, and multithreading. *J. Comput. Chem.* 2010;31:455.
Available:<https://doi.org/10.1002/jcc.21334>
28. Sousa SF, Fernandes PA, Ramos MJ. Protein-ligand docking: current status and future Challenges. *Proteins.* 2006;65:15
Available:<https://doi.org/10.1002/prot.21082>
29. Forli S, Huey R, Pique ME, Sanner MF, Goodsell DS, Olson AJ. Computational protein-ligand docking and virtual drug screening with the AutoDock suite. *J. Nat. Protoc.* 2016;11:905..
Available:<https://doi.org/10.1038/nprot.2016.051>
30. Morris GM, Goodsell DS, Halliday RS, Huey R, Hart WE, Belew RK et al. Automated docking using a Lamarckian genetic algorithm and an empirical binding free energy function. *J. Comput. Chem.* 1998;19:1639.
Available:[https://doi.org/10.1002/\(SICI\)1096-987X\(19981115\)19:14<1639::AID-JCC10>3.0.CO;2-B](https://doi.org/10.1002/(SICI)1096-987X(19981115)19:14<1639::AID-JCC10>3.0.CO;2-B)
31. Lin F-Y, Liu C-I, Liu Y-L, Zhang Y, Wang K, Jeng W-Y et al. 2010 Mechanism of action and inhibition of dehydrosqualene synthase *Proc. Natl. Acad. Sci.* **107** 21337.
Available:<https://doi.org/10.1073/pnas.1010907107>
32. Daina A, Zoete V 2016 A BOILED-Egg To Predict Gastrointestinal Absorption and Brain Penetration of Small Molecules *ChemMedChem***11** 1117.
Available:<https://doi.org/10.1002/cmdc.201600182>
33. Daina A, Michielin O, Zoete V. A Simple, Robust, and Efficient Description of n-Octanol/Water Partition Coefficient for Drug Design Using the GB/SA Approach. *J. Chem. Inf. Model.*2014;54: 3284.
Available:<https://doi.org/10.1021/ci500467k>
34. Hollenberg PF. Characteristics and common properties of inhibitors, inducers, and activators of CYP enzymes. *Drug Metab. Rev.* 2002;34:17.
Available:<https://doi.org/10.1081/dmr-120001387>
35. Zanger UM, Schwab M. Cytochrome P450 enzymes in drug metabolism: Regulation of gene expression, enzyme activities, and impact of genetic variation. *Pharmacol. Ther.* 2013;138:103.
Available:<https://doi.org/10.1016/j.pharmthera.2012.12.007>
36. Hernández-Vázquez, Eduardo Chávez-Riveros, Alejandra Romo-Pérez, Adriana Ramírez-Apán, María Teresa Chávez-Blanco, Alma D. Morales-Bárceñas, Rocío Dueñas González, Alfonso Miranda, Luis D. Cytotoxic Activity and Structure–Activity Relationship of Triazole-Containing Bis(Aryl Ether) Macrocycles. *ChemMed Chem.* 2018;13:1193

- Available:<https://doi.org/10.1002/cmdc.201800075>
37. BinyBalanD.Bahulayan. A novel green synthesis of α/β -amino acid functionalized pyrimidinone peptidomimetics using triazole ligation through click-multi-component reactions. *Tetrahedron Lett.* 2014;55:227. Available:<https://doi.org/10.1016/j.tetlet.2013.11.002>
38. Vendrusculo V, de Souza VP, M. Fontoura LA, M. D'Oca MG, Banzato TP, Monteiro PA et al. Synthesis of novel perillyl–dihydropyrimidinone hybrids designed for antiproliferative activity. *MedChemComm.* 2018;9:1553.
- Available:<https://doi.org/10.1039/c8md00270c>
39. Liu C-I, Liu GY, Song Y, Yin F, Hensler ME, Jeng W-Y et al. A Cholesterol Biosynthesis Inhibitor Blocks &em>Staphylococcus aureus. *Virulence.* *Science.* 2008;319:1391. Available:<https://doi.org/10.1126/science.1153018>
40. Daina A, Michielin O, Zoete V. SwissADME. A free web tool to evaluate pharmacokinetics, drug-likeness and medicinal chemistry friendliness of small molecules. *Sci Rep.* 2017;7:42717. Available:<https://doi.org/10.1038/srep42717>

© 2021 Maddali et al.; This is an Open Access article distributed under the terms of the Creative Commons Attribution License (<http://creativecommons.org/licenses/by/4.0>), which permits unrestricted use, distribution, and reproduction in any medium, provided the original work is properly cited.

Peer-review history:

The peer review history for this paper can be accessed here:
<https://www.sdiarticle5.com/review-history/79023>